6002 *Organometallics* **2010,** *29,* 6002–6011
DOI: 10.1021/om100757e

ORGANOMETALLICS
Article

Mechanistic Study on the Gas-Phase Generation of "Rollover"-Cyclometalated $[M(bipy - H)]^+$ (M = Ni, Pd, Pt)[†]

Burkhard Butschke and Helmut Schwarz*

Institut für Chemie, Technische Universität Berlin, Strasse des 17. Juni 135, D-10623 Berlin, Germany

Received August 3, 2010

"Rollover"-cyclometalated $[Pt(bipy-H)]^+$ (bipy = 2,2′-bipyridine) can be easily generated in the gas phase via HX elimination brought about by collision-induced dissociation (CID) of the cationic complexes $[Pt(X)(bipy)]^+$ with X = CH_3, Cl; the latter as well as other $[M(X)(bipy)]^+$ complexes (M = Ni, Pd; X = CH_3, F, Cl, Br, I, OAc) are accessible by electrospray ionization mass spectrometry. For the nickel and palladium methyl complexes $[M(CH_3)(bipy)]^+$, upon CID, no cyclometalation occurs; rather, homolytic cleavage of the $M-CH_3$ bond takes place. The related chloro complexes $[M(Cl)(bipy)]^+$ (M = Ni, Pd) undergo competitive eliminations of HCl and Cl upon CID, and the branching ratios depend strongly on the collision energy. On the basis of DFT calculations, this metal- and ligand-controlled behavior is a consequence of the rather different energetic requirements for the direct loss of X versus elimination of HX (X = CH_3, Cl). Deuterium-labeling experiments reveal that formation of CH_4 and HCl is only for the platinum complexes due to a genuine "rollover" cyclometalation process, i.e., selective abstraction of a hydrogen atom from the C(3)-position of bipy. In the series of halo-substituted complexes $[Ni(X)(bipy)]^+$ (X = F, Cl, Br, I), the Ni−X bond strength decreases in the sequence F > Cl > Br > I. For X = F, one observes the elimination of HF, which benefits from the particular stability of this molecule; the hydrogen atom in HF is mostly (> 90%) abstracted from position C(6) with < 10% originating from C(3) of the bipy ligand; thus, for this system "rollover" cyclometalation occurs only to a small amount. $[Ni(Cl)(bipy)]^+$ undergoes competitive losses of HCl and Cl upon collision with Xe, and for X = Br and I only homolytic Ni−X bond cleavage takes place. In the elimination of HCl from $[Ni(Cl)(bipy)]^+$, > 60% of the hydrogen atoms originate from C(3), and the remaining from C(4,5,6), as inferred from deuterium-labeling experiments. The acetate complexes $[Ni(OAc)(bipy)]^+$ and $[Pd(OAc)(bipy)]^+$ exhibit eliminations of neutral $AcO^\bullet$, and at elevated collision energies, decarboxylation occurs. C−H bond activation resulting in the formation of HOAc is absent at the detection limit.

Introduction

Among the plethora of organometallic compounds, cyclometalated transition-metal complexes[1] are extremely versatile not only because of their photoluminescent and electronic properties.[2] In fact, they are also used as metallomesogens[3] or as building blocks for supramolecular architectures;[4] further, they are encountered as intermediates in different metal-mediated organic transformations, such as the Heck reaction or the Suzuki coupling,[5] and can be employed in the synthesis of

---

[†] Dedicated to Professor H.-J. Freund on the occasion of his 60th birthday.

*To whom correspondence should be addressed. Fax: (+49) 30-314-21102. E-mail: Helmut.Schwarz@mail.chem.tu-berlin.de.

(1) (a) Cope, A. C.; Siekman, R. W. *J. Am. Chem. Soc.* **1965**, *87*, 3272. (b) Dehand, J.; Pfeffer, M. *Coord. Chem. Rev.* **1976**, *18*, 327. (c) Bruce, M. I. *Angew. Chem., Int. Ed. Engl.* **1977**, *16*, 73. (d) Omae, I. *Chem. Rev.* **1979**, *79*, 287. (e) Omae, I. *Coord. Chem. Rev.* **1980**, *32*, 235. (f) Constable, E. C. *Polyhedron* **1984**, *3*, 1037. (g) Rothwell, I. P. *Polyhedron* **1985**, *4*, 177. (h) Ryabov, A. D. *Chem. Rev.* **1990**, *90*, 403. (i) Albrecht, M.; van Koten, G. *Angew. Chem., Int. Ed.* **2001**, *40*, 3750. (j) van der Boom, M. E.; Milstein, D. *Chem. Rev.* **2003**, *103*, 1759. (k) Omae, I. *Coord. Chem. Rev.* **2004**, *248*, 995. (l) Mohr, F.; Privér, S. H.; Bhargava, S. K.; Bennett, M. A. *Coord. Chem. Rev.* **2006**, *250*, 1851. (m) Albrecht, M. *Chem. Rev.* **2010**, *110*, 576.

(2) (a) Lai, S.-W.; Cheung, T.-C.; Chan, M. C. W.; Cheung, K.-K.; Peng, S.-M.; Che, C.-M. *Inorg. Chem.* **2000**, *39*, 255. (b) Ma, B.; Djurovich, P. I.; Thompson, M. E. *Coord. Chem. Rev.* **2005**, *249*, 1501. (c) Ghedini, M.; Aiello, I.; Crispini, A.; Golemme, A.; La Deda, M.; Pucci, D. *Coord. Chem. Rev.* **2006**, *250*, 1373. (d) Lowry, M. S.; Bernhard, S. *Chem.—Eur. J.* **2006**, *12*, 7970. (e) Wu, L.-L.; Yang, C.-H.; Sun, I.-W.; Chu, S.-Y.; Kao, P.-C.; Huang, H.-H. *Organometallics* **2007**, *26*, 2017. (f) Kui, S. C. F.; Sham, I. H. T.; Cheung, C. C. C.; Ma, C.-W.; Yan, B.; Zhu, N.; Che, C.-M.; Fu, W.-F. *Chem.—Eur. J.* **2007**, *13*, 417. (g) Zucchi, G.; Maury, O.; Thuéry, P.; Gumy, F.; Bünzli, J.-C. G.; Ephritikhine, M. *Chem.—Eur. J.* **2009**, *15*, 9686.

(3) (a) Pucci, D.; Barberio, G.; Bellusci, A.; Crispini, A.; Ghedini, M. *J. Organomet. Chem.* **2006**, *691*, 1138. (b) Marcos, M. In *Metallomesogens*; José Luis, S., Ed.; Wiley-VCH: Germany, 2007; p 235.

(4) (a) Huck, W. T. S.; Hulst, R.; Timmerman, P.; van Veggel, F. C. J. M.; Reinhoudt, D. N. *Angew. Chem., Int. Ed.* **1997**, *36*, 1006. (b) Hall, J. R.; Loeb, S. J.; Shimizu, G. K. H.; Yap, G. P. A. *Angew. Chem., Int. Ed.* **1998**, *37*, 121. (c) Huck, W. T. S.; Prins, L. J.; Fokkens, R. H.; Nibbering, N. M. M.; van Veggel, F. C. J. M.; Reinhoudt, D. N. *J. Am. Chem. Soc.* **1998**, *120*, 6240. (d) Carina, R. F.; Williams, A. F.; Bernardinelli, G. *Inorg. Chem.* **2001**, *40*, 1826. (e) Lopez-Torres, M.; Fernandez, A.; Fernandez, J. J.; Suarez, A.; Castro-Juiz, S.; Vila, J. M.; Pereira, M. T. *Organometallics* **2001**, *20*, 1350. (f) Slagt, M. Q.; van Zwieten, D. A. P.; Moerkerk, A. J. C. M.; Gebbink, R. J. M. K.; van Koten, G. *Coord. Chem. Rev.* **2004**, *248*, 2275. (g) Lu, W.; Roy, V. A. L.; Che, C.-M. *Chem. Commun.* **2006**, 3972. (h) Gagliardo, M.; Rodríguez, G.; Dam, H. H.; Lutz, M.; Spek, A. L.; Havenith, R. W. A.; Coppo, P.; De Cola, L.; Hartl, F.; van Klink, G. P. M.; van Koten, G. *Inorg. Chem.* **2006**, *45*, 2143.

(5) (a) Xiong, Z.; Wang, N.; Dai, M.; Li, A.; Chen, J.; Yang, Z. *Org. Lett.* **2004**, *6*, 3337. (b) Frey, G. D.; Schutz, J.; Herdtweck, E.; Herrmann, W. A. *Organometallics* **2005**, *24*, 4416. (c) Mulcahy, S. P.; Carroll, P. J.; Meggers, E. *Tetrahedron Lett.* **2006**, *47*, 8877.

various heterocyclic products.[6] The majority of these organometallic compounds contain a group 10 metal, with palladium being the most versatile one,[7] followed by platinum and then nickel. Also Mn, Fe, Co, Ru, Rh, Os, and Ir are popular transition metals for cyclometalation reactions, and recently the synthesis of the first "rollover"-cyclometalated gold complex was reported.[8] Quite a few mechanistic studies, dealing with the formation of cyclometalated compounds, were conducted during the last decades, addressing electronic aspects,[9] the influence of the transition metal,[10] or the effect of the donor atom that is coordinated to the metal center.[11] However, mechanistic studies of the so-called "rollover" cyclometalation,[12] where decomplexation and rotation of a heteroaryl ring constitute prerequisites for a metal-mediated activation of a C−H bond, are quite rare, and there are only very few comparative studies for cyclometalation reactions of the group 10 metals Ni, Pd, and Pt.[13] Gas-phase experiments are ideally suited to probe the intrinsic features of a chemical reaction in contrast to solution-phase experiments, which—by definition—are obscured by often ill-defined solvent and aggregation effects as well as the influence of counterions. Earlier, we have reported in quite some detail on the gas-phase generation of "rollover"-cyclometalated $[Pt(bipy - H)]^+$ (**2-Pt**; Chart 1) starting from the corresponding platinum-methyl complexes $[Pt(CH_3)(bipy)((CH_3)_2S)]^+$ and $[Pt(CH_3)(bipy)]^+$ (**1-PtMe**).[14] In the present study, we extend this work to the nickel and palladium complexes, **2-Ni** and **2-Pd**, respectively; moreover, we were interested to probe whether or not halogens, especially chlorine, are also adequate ligands for the formation of **2** via an intramolecular C−H bond activation. In addition, mechanistic aspects are addressed; for example, are we dealing with an OA/RE (oxidative addition/reductive elimination) or rather a metathesis scenario in the "rollover" cyclometalation to generate **2** and HX for the different metals M = Ni, Pd, Pt and the ligands X = CH_3, Cl?[15] Furthermore, as many synthetic procedures for the generation of cyclometalated palladium complexes are based on the use of palladium acetate,[1h,7a,9c,16] **1-PdOAc** has been included in our investigations and compared with **1-NiOAc** in order to study if X = OAc can also serve as a suitable precursor ligand for the formation of "rollover"-cyclometalated transition-metal complexes in the gas phase.

Chart 1. Overview of the Relevant Structural Units $[M(X)(bipy)]^+$ (1 = 1-MX), $[M(bipy - H)]^+$ (2 = 2-M), and $[M(bipy)]^+$ (3 = 3-M) with M = Ni, Pd, Pt and X = CH_3, F, Cl, Br, I, OAc As Well As of the Deuterated 2,2′-Bipyridine Ligands [3,3′-D_2]-bipy and [6,6′-D_2]-bipy Used in This Study

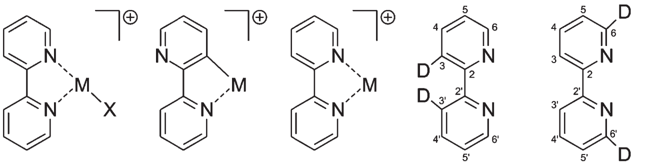

1 **2** **3** [3,3′-D_2]-bipy [6,6′-D_2]-bipy

Table 1. Overview of the *m/z* Values That Were Chosen for Mass Selection in Order to Produce a [D_2]-Enriched $[M(X)(bipy)]^+$ Ion Beam (M = Ni, Pd, Pt; X = CH_3, Cl, F) Together with the Resulting [D_0], [D_1], and [D_2] Fractions (given in %)

	m/z	[D_0]	[D_1]	[D_2]
[3,3′-D_2]-**1-NiCl**	251[a]	2	3	95
[6,6′-D_2]-**1-NiCl**	251[a]	3	1	96
[3,3′-D_2]-**1-PdCl**	301[b]	1	3	96
[6,6′-D_2]-**1-PdCl**	301[b]	2	1	97
[3,3′-D_2]-**1-PtCl**	391[c]	0	3	97
[3,3′-D_2]-**1-PtMe**	369[d]	1	3	96
[3,3′-D_2]-**1-NiF**	235[e]	1	0	99
[6,6′-D_2]-**1-NiF**	235[e]	2	1	97

[a] The [D_2] fraction of the signal contains exclusively [D_2]-**1-^{58}Ni^{35}Cl**. [b] The [D_2] fraction of the signal contains [D_2]-**1-^{108}Pd^{35}Cl** (74%), [D_2]-**1-^{106}Pd^{37}Cl** (24%), and a small amount of ^{13}C-containing [D_2]-**1-^{105}Pd^{37}Cl** (2%). [c] The [D_2] fraction of the signal contains [D_2]-**1-^{198}Pt^{35}Cl** (44%), [D_2]-**1-^{196}Pd^{37}Cl** (49%), and ^{13}C-containing [D_2]-**1-^{195}Pt^{37}Cl** (7%). [d] The [D_2] fraction of the signal contains [D_2]-**1-^{196}PtMe** (87%) and ^{13}C containing [D_2]-**1-^{195}PtMe** (13%) (but only 1.3% [D_2]-**1-^{195}Pt^{13}CH$_3$**). [e] The [D_2] fraction of the signal contains exclusively [D_2]-**1-^{58}NiF**.

Here, we present the results for the gas-phase fragmentations of $[M(CH_3)(bipy)]^+$ and $[M(Cl)(bipy)]^+$ (M = Ni, Pd, Pt; bipy = 2,2′-bipyridine), $[Ni(X)(bipy)]^+$ (X = F, Cl, Br, I), and $[M(OAc)(bipy)]^+$ (M = Ni, Pd) generated via electrospray ionization (ESI).[17] 2,2′-Bipyridine has been chosen not only because bipy and related heterocyclic systems represent versatile ligands in the coordination chemistry of transition-metal complexes[18] but bipy possesses the potential to bring about "rollover" cyclometalation.[12,14] Labeling experiments have been conducted to trace the origin of the hydrogen atom

---

[6] (a) Pfeffer, M. *Pure Appl. Chem.* **1992**, *64*, 335. (b) Vicente, J.; Abad, J.-A.; Bergs, R.; Jones, P. G.; Ramirez de Arellano, M. C. *Organometallics* **1996**, *15*, 1422. (c) Ferstl, W.; Sakodinskaya, I. K.; Beydoun-Sutter, N.; Le Borgne, G.; Pfeffer, M.; Ryabov, A. D. *Organometallics* **1997**, *16*, 411. (d) Hwang, S. J.; Cho, S. H.; Chang, S. *J. Am. Chem. Soc.* **2008**, *130*, 16158. (e) Hull, K. L.; Sanford, M. S. *J. Am. Chem. Soc.* **2009**, *131*, 9651.

[7] (a) Ryabov, A. D. *Synthesis* **1985**, 233. (b) Dupont, J.; Pfeffer, M.; Spencer, J. *Eur. J. Inorg. Chem.* **2001**, *2001*, 1917.

[8] Cocco, F.; Cinellu, M. A.; Minghetti, G.; Zucca, A.; Stoccoro, S.; Maiore, L.; Manassero, M. *Organometallics* **2010**, *29*, 1064.

[9] (a) Bruce, M. I.; Gardner, R. C. F.; Stone, F. G. A. *J. Chem. Soc., Dalton Trans.* **1976**, 81. (b) Takahashi, H.; Tsuji, J. *J. Organomet. Chem.* **1967**, *10*, 511. (c) Canty, A. J.; van Koten, G. *Acc. Chem. Res.* **1995**, *28*, 406. (d) Owen, J. S.; Labinger, J. A.; Bercaw, J. E. *J. Am. Chem. Soc.* **2004**, *126*, 8247. (e) Li, L.; Brennessel, W. W.; Jones, W. D. *Organometallics* **2009**, *28*, 3492.

[10] Bruce, M. I.; Goodall, B. L.; Stone, F. G. A. *J. Chem. Soc., Chem. Commun.* **1973**, 558.

[11] Parshall, G. W. *Acc. Chem. Res.* **1970**, *3*, 139.

[12] (a) Wickramasinghe, W. A.; Bird, P. H.; Serpone, N. *J. Chem. Soc., Chem. Commun.* **1981**, 1284. (b) Constable, E. C.; Seddon, K. R. *J. Chem. Soc., Chem. Commun.* **1982**, 34. (c) Nord, G.; Hazell, A. C.; Hazell, R. G.; Farver, O. *Inorg. Chem.* **1983**, *22*, 3429. (d) Spellane, P. J.; Watts, R. J.; Curtis, C. J. *Inorg. Chem.* **1983**, *22*, 4060. (e) Dholakia, S.; Gillard, R. D.; Wimmer, F. L. *Inorg. Chim. Acta* **1983**, *69*, 179. (f) Braterman, P. S.; Heath, G. A.; MacKenzie, A. J.; Noble, B. C.; Peacock, R. D.; Yellowlees, L. J. *Inorg. Chem.* **1984**, *23*, 3425. (g) Skapski, A. C.; Sutcliffe, V. F.; Young, G. B. *J. Chem. Soc., Chem. Commun.* **1985**, 609. (h) Minghetti, G.; Doppiu, A.; Zucca, A.; Stoccoro, S.; Cinellu, M.; Manassero, M.; Sansoni, M. *Chem. Heterocycl. Compd.* **1999**, *35*, 992. (i) Zucca, A.; Doppiu, A.; Cinellu, M. A.; Stoccoro, S.; Minghetti, G.; Manassero, M. *Organometallics* **2002**, *21*, 783. (j) Minghetti, G.; Stoccoro, S.; Cinellu, M. A.; Soro, B.; Zucca, A. *Organometallics* **2003**, *22*, 4770. (k) Zucca, A.; Cinellu, M. A.; Minghetti, G.; Stoccoro, S.; Manassero, C. *Eur. J. Inorg. Chem.* **2004**, 4484. (l) Stoccoro, S.; Zucca, A.; Petretto, G. L.; Cinellu, M. A.; Minghetti, G.; Manassero, M. *J. Organomet. Chem.* **2006**, *691*, 4135. (m) Minghetti, G.; Stoccoro, S.; Cinellu, M. A.; Petretto, G. L.; Zucca, A. *Organometallics* **2008**, *27*, 3415. (n) Zucca, A.; Petretto, G. L.; Stoccoro, S.; Cinellu, M. A.; Manassero, M.; Manassero, C.; Minghetti, G. *Organometallics* **2009**, *28*, 2150.

[13] Piro, N. A.; Owen, J. S.; Bercaw, J. E. *Polyhedron* **2004**, *23*, 2797.

[14] (a) Butschke, B.; Schlangen, M.; Schröder, D.; Schwarz, H. *Chem.—Eur. J.* **2008**, *14*, 11050. (b) Butschke, B.; Schröder, D.; Schwarz, H. *Organometallics* **2009**, *28*, 4340.

[15] For a detailed discussion of various mechanistic scenarios of gas-phase organometallic transformations, see: Armélin, M.; Schlangen, M.; Schwarz, H. *Chem.—Eur. J.* **2008**, *14*, 5229.

[16] (a) Gomez, M.; Granell, J.; Martinez, M. *Organometallics* **1997**, *16*, 2539. (b) Gómez, M.; Granell, J.; Martinez, M. *J. Chem. Soc., Dalton Trans.* **1998**, 37. (c) Davies, D. L.; Donald, S. M. A.; Macgregor, S. A. *J. Am. Chem. Soc.* **2005**, *127*, 13754.

[17] http://nobelprize.org/chemistry/laureates/2002/.

[18] (a) Togni, A.; Venanzi, L. M. *Angew. Chem., Int. Ed. Engl.* **1994**, *33*, 497. (b) Himeda, Y.; Onozawa-Komatsuzaki, N.; Miyazawa, S.; Sugihara, H.; Hirose, T.; Kasuga, K. *Chem.—Eur. J.* **2008**, *14*, 11076.

Table 2. Major Fragments in the CID of Mass-Selected [M(CH_3)(bipy)]$^+$ (1-MMe) Complexes (M = Ni, Pd, Pt) at Various Collision Energies (E_{lab} in eV)[a]

	E_{lab}	**1-MMe**	− CH_3	− CH_4	− bipy	− CH_3/bipy	− MCH_2	− [M,C,H_3]	− [M,C,H_4]
1-NiMe	0	100	*87*						
	5	24	*100*						
	10	24	*100*						
	15	41	*100*			*3*			
	20	48	*100*		*8*	*14*			
	25	72	*100*		*27*	*45*			
1-PdMe	0	100	*22*	**2**					
	5	52	*100*	**4**					
	10	16	*100*	**3**		*>0*			
	15	22	*100*	**1**	*3*	*9*		3	**2**
	20	41	*100*		*24*	*41*		10	**9**
	25	52	*100*		*69*	*80*		12	**17**
1-PtMe	0	100		**44**			1		
	5	68		**100**			15		
	10	58		**100**			49		
	15	29		**81**			100		
	20	17		**36**			100		
	25	19		**22**			100		

[a] Relative intensities are normalized to the base peak = 100. Numbers given in bold involve intramolecular C−H bond activation processes. Numbers in italics indicate simple ligand-loss processes.

involved in the formation of HX. Finally, DFT-based calculations were performed to provide insight in those mechanistic aspects of the C−H bond activation that are not directly accessible from the experiments.

Experimental and Computational Details

The present experiments were performed with a VG BIO-Q mass spectrometer of QHQ configuration (Q: quadrupole, H: hexapole) equipped with an ESI source as described in detail previously.[19] In brief, millimolar solutions of various precursors in pure methanol, ethanol, or acetonitrile (see below for more details) were introduced through a fused-silica capillary to the ESI source via a syringe pump (ca. 3 μL min^{-1}) in order to produce the ligated metal cations under investigation. Nitrogen was used as a nebulizing and drying gas at a source temperature of 80 °C. Maximal yields of the desired complexes were achieved by adjusting the cone voltage (U_c) between 50 and 70 V; U_c determines the degree of collisional activation of the incident ions in the transfer from the ESI source to the mass spectrometer.[20] The identity of the ions was confirmed by comparison with the expected isotope patterns.[21] The isotope pattern also assisted in the choice of the adequate precursor ion in order to avoid coincidental mass overlaps of isobaric species in the mass-selected ion beam.[22] Collision-induced dissociation experiments were probed at different collision energies E_{lab} between 0 and 25 eV, and the intensities of all ions were normalized to the base-peak intensity, which was set to 100%.

For the generations of [Pd(CH_3)(bipy)]$^+$ and [Pt(CH_3)(bipy)]$^+$ millimolar solutions of [Pd(CH_3)$_2$(tmeda)][23] (tmeda = *N*,*N*,*N*′,*N*′-tetramethylethylenediamine) and [Pt(CH_3)$_2$(μ-(CH_3)$_2$S)]$_2$,[24] respectively, and 2,2′-bipyridine in methanol were used. As [Ni(CH_3)$_2$(bipy)], prepared according to ref 25 starting from commercially available [Ni(CH_3)$_2$(tmeda)], is extremely sensitive to protic solvents, the green solid was dissolved in dry acetonitrile to give a nearly colorless solution; ESI of this solution produced [Ni(CH_3)(bipy)]$^+$. For the preparation of [Pd(Cl)$_2$(bipy)], equimolar amounts of $PdCl_2$ and bipy were stirred at room temperature in methanol for 6 h and the beige precipitate was filtered; [Pt(Cl)$_2$(bipy)] was synthesized according to ref 26. Both chloride complexes are nearly insoluble in methanol and only slightly better in acetonitrile. However, [Pd(Cl)(bipy)]$^+$ and [Pt(Cl)(bipy)]$^+$ cannot be produced via ESI of the acetonitrile solutions. Therefore, equimolar acetonitrile solutions of the chloride complexes and of AgOTf were mixed in order to substitute one chloride anion for the weakly coordinating triflate counterion. Electrospray ionization of these solutions yielded the desired species. [Ni(X)(bipy)]$^+$ (X = Cl, Br, I) cations can be easily generated from methanolic solutions of [Ni(X)$_2$(bipy)], which precipitates from a mixture of equimolar ethanolic solutions of the corresponding nickel halide and 2,2′-bipyridine at room temperature. [Ni(F)$_2$(bipy)] cannot be generated in this way; rather, [Ni(F)(bipy)]$^+$ was generated via ESI from a diluted solution of NiF_2 and bipy in ethanol. ESI of millimolar solutions of [Ni(OAc)$_2$] or [Pd(OAc)$_2$] together with 2,2′-bipyridine in methanol produced [M(OAc)(bipy)]$^+$ (M = Ni, Pd). For the deuterium-labeling experiments [3,3′-D_2]-2,2′-bipyridine ([3,3′-D_2]-bipy) and [6,6′-D_2]-2,2′-bipyridine ([6,6′-D_2]-bipy) were employed. [3,3′-D_2]-bipy was prepared through palladium-mediated coupling (see ref 27) of 2-chloro-3-deuteropyridine synthesized according to ref 28. Based on a mass spectrometric analysis, a labeling distribution of [D_0]:[D_1]:[D_2] = 2:19:79 was obtained. [6,6′-D_2]-bipy was synthesized via lithiation of 6,6′-dibromo-2,2′-bipyridine with *n*-BuLi in THF[29] and subsequent quenching of the reaction mixture with D_2O, resulting in a deuterium distribution of [D_0]:[D_1]:[D_2] = 4:8:88. On the basis of these isotope distributions, [D_2]-[M(X)(bipy)]$^+$ complexes (M = Ni, Pd, Pt; X = CH_3, Cl, F) could be produced in at least 95% purity when the appropriate peak was mass-selected. A summary of the precursor ions that were used for mass selection and the deuterium incorporation for the various complexes is given in Table 1. In the case where the mass-selected signal consisted of

---

(19) (a) Schröder, D.; Weiske, T.; Schwarz, H. *Int. J. Mass Spectrom.* **2002**, *219*, 729. (b) Trage, C.; Schröder, D.; Schwarz, H. *Chem.—Eur. J.* **2005**, *11*, 619.

(20) Cech, N. B.; Enke, C. G. *Mass Spectrom. Rev.* **2001**, *20*, 362.

(21) http://www.sisweb.com/mstools/isotope.htm.

(22) Schröder, D.; Schwarz, H. *Can. J. Chem.* **2005**, *83*, 1936.

(23) Biscoe, M. R.; Fors, B. P.; Buchwald, S. L. *J. Am. Chem. Soc.* **2008**, *130*, 6686.

(24) Hill, G. S.; Irwin, M. J.; Levy, C. J.; Rendina, L. M.; Puddephatt, R. J.; Andersen, R. A.; Mclean, L. In *Inorganic Syntheses*; Marcetta, Y. D., Eds.; Wiley: New York, 1998; p 149.

(25) Kaschube, W.; Pörschke, K. R.; Wilke, G. *J. Organomet. Chem.* **1988**, *355*, 525.

(26) Egan, T. J.; Koch, K. R.; Swan, P. L.; Clarkson, C.; Van Schalkwyk, D. A.; Smith, P. J. *J. Med. Chem.* **2004**, *47*, 2926.

(27) Bamfield, P.; Quan, P. M. *Synthesis* **1978**, 537.

(28) Bérillon, L.; Leprêtre, A.; Turck, A.; Plé, N.; Quéguiner, G.; Cahiezc, G.; Knochel, P. *Synlett* **1998**, 1359.

(29) Parks, J. E.; Wagner, B. E.; Holm, R. H. *J. Organomet. Chem.* **1973**, *56*, 53.

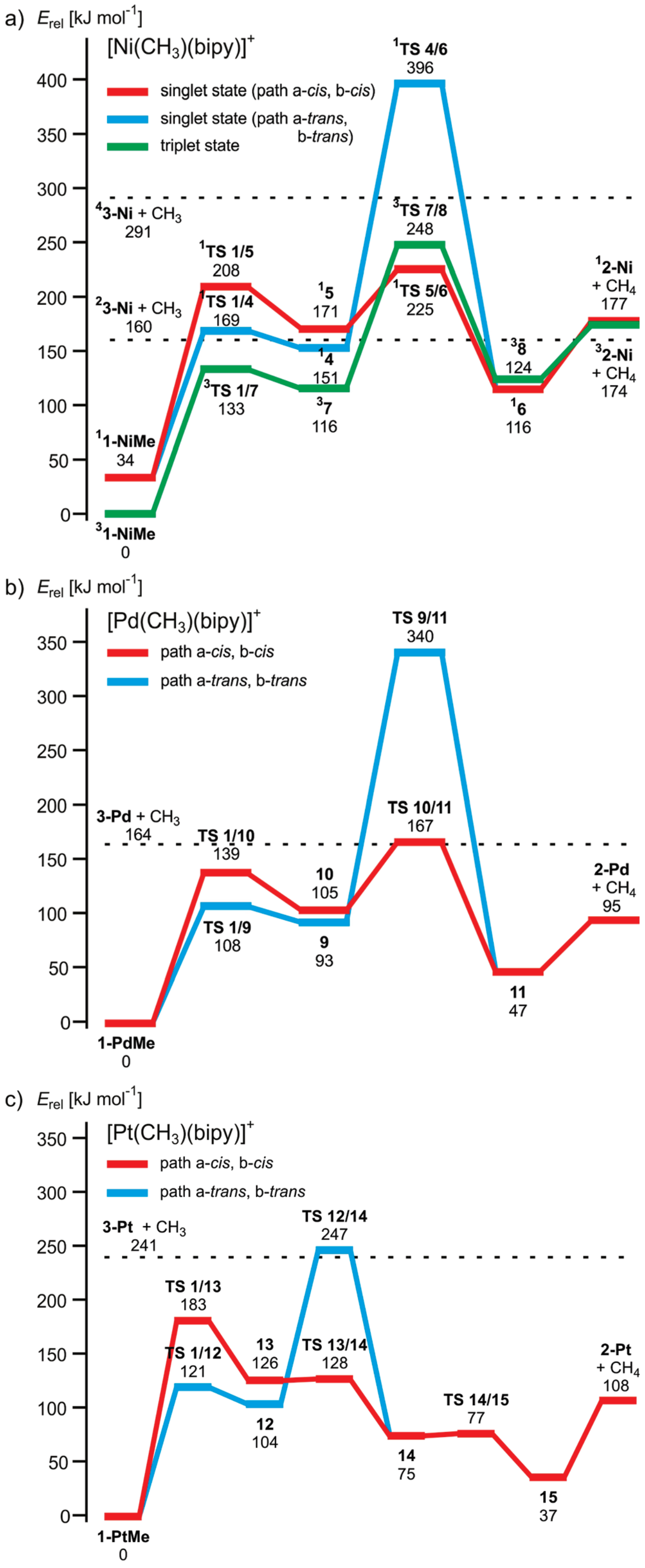

Figure 1. Schematic PESs for the fragmentations of $[\mathrm{M(CH_3)(bipy)}]^+$ (M = Ni, Pd, Pt) according to $[\mathrm{M(CH_3)(bipy)}]^+$ (**1-MMe**) → $[\mathrm{M(bipy - H)}]^+$ (**2**) + CH_4 and $[\mathrm{M(CH_3)(bipy)}]^+$ (**1-MMe**) → $[\mathrm{M(bipy)}]^+$ (**3**) + CH_3 based on DFT calculations using the B3LYP functional. For further explanations, see Scheme 1 and text.

^{35}Cl- and ^{37}Cl-containing species, only the signals for the losses of $H^{37}Cl$ and $D^{37}Cl$ were considered in the evaluation of the CID results, as only for these signals can an overlap with isobaric fragmentation products be excluded.

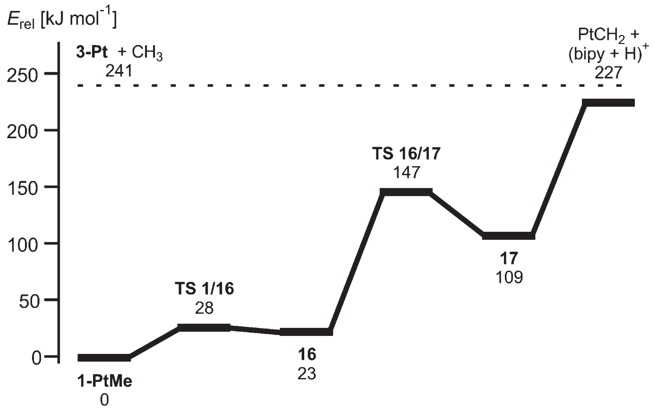

Figure 2. Schematic PES for the fragmentation of $[\mathrm{Pt(CH_3)(bipy)}]^+$ according to $[\mathrm{Pt(CH_3)(bipy)}]^+$ (**1-PtMe**) → $(\mathrm{bipy + H})^+$ + $PtCH_2$ and $[\mathrm{Pt(CH_3)(bipy)}]^+$ (**1-PtMe**) → $[\mathrm{M(bipy)}]^+$ (**3**) + CH_3 based on DFT calculations using the B3LYP functional.

In the computational studies we have employed the Gaussian09 program package[30] using basis sets of approximately triple-ξ quality. For H, C, N, and Cl atoms these were the triple-ξ plus polarization basis sets (TZVP) of Ahlrichs and co-workers.[31] For complexes containing Ni, Pd, and Pt, the Stuttgart−Dresden scalar relativistic pseudopotential was employed in conjunction with the corresponding basis sets.[32] The fragmentation pathways for the processes defined in eqs 1 and 2 (M = Ni, Pd, Pt; X = CH_3, Cl) were calculated with the B3LYP[33] functional using the basis sets given above. All energies (given in kJ mol^{-1}) are corrected for (unscaled) zero-point vibrational energy contributions. Intrinsic reaction coordinate (IRC) calculations were performed to link transition-state structures with the respective intermediates.[34] The discussion of the computational findings will be confined to the singlet state of the various platinum and palladium cations, because exploratory calculations revealed that their triplet states are generally much higher in energy for all species investigated and, therefore, are not likely to be involved in the experiments conducted at ambient temperature. However, for the nickel complexes both the singlet and the triplet states must be taken into account.

$$[\mathrm{M(X)(bipy)}]^+\ (\mathbf{1}) \rightarrow [\mathrm{M(bipy - H)}]^+\ (\mathbf{2}) + \mathrm{HX} \tag{1}$$

$$[\mathrm{M(X)(bipy)}]^+\ (\mathbf{1}) \rightarrow [\mathrm{M(bipy)}]^+\ (\mathbf{3}) + \mathrm{X} \tag{2}$$

---

(30) Frisch, M. J.; Trucks, G. W.; Schlegel, H. B.; Scuseria, G. E.; Robb, M. A.; Cheeseman, J. R.; Scalmani, G.; Barone, V.; Mennucci, B.; Petersson, G. A.; Nakatsuji, H.; Caricato, M.; Li, X.; Hratchian, H. P.; Izmaylov, A. F.; Bloino, J.; Zheng, G.; Sonnenberg, J. L.; Hada, M.; Ehara, M.; Toyota, K.; Fukuda, R.; Hasegawa, J.; Ishida, M.; Nakajima, T.; Honda, Y.; Kitao, O.; Nakai, H.; Vreven, T.; Montgomery, J. A.; , Jr., Peralta, J. E.; Ogliaro, F.; Bearpark, M.; Heyd, J. J.; Brothers, E.; Kudin, K. N.; Staroverov, V. N.; Kobayashi, R.; Normand, J.; Raghavachari, K.; Rendell, A.; Burant, J. C.; Iyengar, S. S.; Tomasi, J.; Cossi, M.; Rega, N.; Millam, J. M.; Klene, M.; Knox, J. E.; Cross, J. B.; Bakken, V.; Adamo, C.; Jaramillo, J.; Gomperts, R.; Stratmann, R. E.; Yazyev, O.; Austin, A. J.; Cammi, R.; Pomelli, C.; Ochterski, J. W.; Martin, R. L.; Morokuma, K.; Zakrzewski, V. G.; Voth, G. A.; Salvador, P.; Dannenberg, J. J.; Dapprich, S.; Daniels, A. D.; Ö. Farkas, Foresman, J. B.; Ortiz, J. V.; Cioslowski, J.; Fox, D. J. *Gaussian 09*, Revision A.1; Gaussian, Inc.: Wallingford, CT, 2009.

(31) Schäfer, A.; Huber, C.; Ahlrichs, R. *J. Chem. Phys.* **1994**, *100*, 5829.

(32) (a) Andrae, D.; Häussermann, U.; Dolg, M.; Stoll, H.; Preuss, H. *Theor. Chem. Acc.* **1990**, *77*, 123. (b) Dolg, M.; Stoll, H.; Preuss, H.; Pitzer, R. M. *J. Phys. Chem.* **1993**, *97*, 5852. (c) Peterson, K. A.; Figgen, D.; Dolg, M.; Stoll, H. *J. Chem. Phys.* **2007**, *126*, 124101.

(33) (a) Lee, C.; Yang, W.; Parr, R. G. *Phys. Rev. B* **1988**, *37*, 785. (b) Becke, A. D. *J. Chem. Phys.* **1993**, *98*, 5648.

(34) (a) Fukui, K. *J. Phys. Chem.* **1970**, *74*, 4161. (b) Fukui, K. *Acc. Chem. Res.* **1981**, *14*, 363. (c) Gonzalez, C.; Schlegel, H. B. *J. Phys. Chem.* **1990**, *94*, 5523.

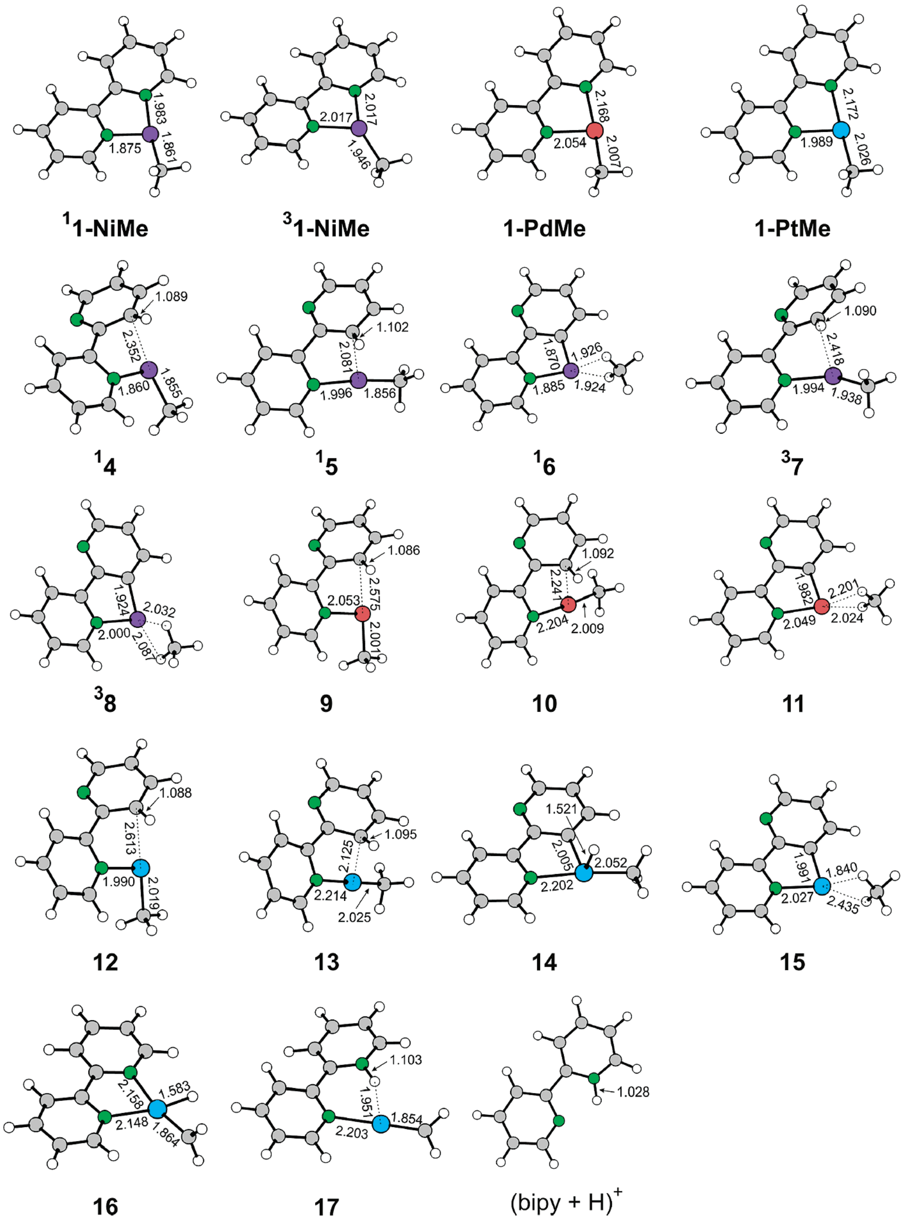

Figure 3. Geometry-optimized minimum structures of the species mentioned in Figures 1 and 2 together with relevant bond lengths (in Å) around the metal cores as calculated with the B3LYP functional.

Results and Discussion

Fragmentation of [M(CH$_3$)(bipy)]$^+$ **(M = Ni, Pd, Pt).** The fragmentation behavior of cationic [Pt(CH$_3$)(L)]$^+$ with L = 2,2′-bipyridine, 2,2′-bipyrimidine (bipyrm), and 1,10-phenanthroline (phen) was already discussed elsewhere.[14b] Upon CID of [Pt(CH$_3$)(bipy)]$^+$ (**1-PtMe**) with xenon, elimination of neutral CH$_4$ occurs even at the lowest collision energies; at elevated collision energies, PtCH$_2$ loss gains in importance (Table 2). In contrast, for [Pt(CH$_3$)(bipyrm)]$^+$ and [Pt(CH$_3$)(phen)]$^+$ no liberation of CH$_4$ takes place at the detection limit of the instrument; these findings already indicate a genuine "rollover" cyclometalation operative in the reaction [Pt(CH$_3$)(bipy)]$^+$ → [Pt(bipy−H)]$^+$ + CH$_4$ because for, L = bipyrm, no hydrogen atoms are available at either the C(3)- or C(3′)-positions, and for L = phen, rotation around a C−C single bond is not possible. When [3,3′-D$_2$]-**1-PtMe** (m/z = 369) is used, the methane eliminated consists of 97% CH$_3$D, thus demonstrating the (near exclusive) occurrence of a "rollover"-cyclometalation process in the fragmentation of **1-PtMe**, i.e., the abstraction of the hydrogen atom from position C(3) of the bipy ligand after initial decomplexation and rotation of a pyridyl ring. Upon CID of [Ni(CH$_3$)(bipy)]$^+$ (**1-NiMe**) and of [Pd(CH$_3$)(bipy)]$^+$ (**1-PdMe**), the most dominant process corresponds to the homolytic cleavage of the M−CH$_3$ bond to liberate the methyl group (Table 2). At elevated collision energies, elimination of the bipy ligand as well as the consecutive eliminations of CH$_3$ and bipy are observed. For **1-NiMe**, at any collision energies employed, CH$_4$ is not formed at all; however, for **1-PdMe** at low collision energies a rather small amount of CH$_4$ is lost. At higher E_{lab} values, the elimination of neutral [Pd,C,H$_4$] occurs; this is also indicative for an intramolecular hydrogen-abstraction process.

DFT calculations were performed for the processes described in eqs 1 and 2 for the complexes [M(CH$_3$)(bipy)]$^+$ (M = Ni, Pd, Pt) aimed at explaining the different fragmentation behavior, i.e., why at low energies is CH$_3$ preferentially lost for M = Ni and Pd but CH$_4$ for M = Pt? The corresponding potential-energy surfaces (PESs) are given in Figure 1, and selected structures are shown in Figure 3 (the full set of structures is available in the Supporting Information). Starting from **1**, after decomplexation, rotation of a pyridyl ring constitutes a prerequisite for the eventual activation of the C(3)−H bond concomitant with the formation of **2** and HX. As in the singlet-state structures of $[M(CH_3)(bipy)]^+$ (**1-MMe**), for M = Ni, Pd, and Pt, the metal center has a nearly square-planar coordination sphere (with one vacant coordination site), there are two options: rotation of the pyridyl ring oriented *cis* or *trans* to the methyl group (path a-*cis* or path a-*trans*, respectively, in Scheme 1; note that in all structural representations the upper pyridyl ring is displayed as rotated). Due to a *trans* effect of the methyl group, the M−N interaction *trans* to the CH_3 ligand is weakened. This becomes obvious upon inspection of the starting structures **^{1}1-NiMe**, **1-PdMe**, and **1-PtMe**, where the M−N bond lengths *trans* to the methyl group are 0.108, 0.114, and 0.183 Å longer than those M−N bonds that are alligned *cis* to the CH_3 ligand. Therefore, the rotation of the ring *trans* to the methyl group (**^{1}1-NiMe** → **^{1}4**, **1-PdMe** → **9**, and **1-PtMe** → **12** in Figures 1 and 3; **1** → **1′-*trans*** in Scheme 1) is facilitated by 39, 31, and 62 kJ mol^{-1}, respectively, compared with the rotation of the ring *cis* to the methyl group (leading to the **1′-*cis*** structures **^{1}5**, **10**, and **13**, respectively). For $[Ni(CH_3)(bipy)]^+$, the triplet-state structure **^{3}1-NiMe** is 34 kJ mol^{-1} more favorable than the singlet-state structure **^{1}1-NiMe**; due to the C_s symmetry of **^{3}1-NiMe**, rotations of both rings (via **^{3}TS 1/7**, see SI 1) are equivalent. After rotation of the pyridyl ring, the metal center interacts with the C(3)−H bond and CH_4 can be formed either in a σ-bond metathesis scenario for M = Ni and Pd or via an OA/RE (oxidative addition/reductive elimination) mechanism for M = Pt.[15] Also in the C−H bond activation step, the *trans* effect of the methyl group affects the energetic requirements. This is further reflected in the geometric features of the **1′-*trans*** structures **^{1}4**, **9**, and **12** as compared to the **1′-*cis*** structures **^{1}5**, **10**, and **13**: in the **1′-*trans*** structures, the M−C(3) distance is increased by 0.271, 0.334, and 0.488 Å and, more importantly, the C(3)−H bond distance is decreased by 0.013, 0.006, and 0.007 Å for the Ni-, Pd-, and Pt-containing structures, when compared with the respective **1′-*cis*** structures. Thus, the interaction of the metal center with the C(3)−H bond is weaker in the **1′-*trans*** complexes, and C−H bond activation via **^{1}TS 4/6**, **TS 9/11**, and **TS 12/14** is energetically more demanding by 171, 173, and 119 kJ mol^{-1} for M = Ni, Pd, and Pt, respectively, as compared with the corresponding **1′-*cis*** structures. For the C−H bond activation step in the fragmentation of the triplet-state species **^{3}1-NiMe**, only one transition state, **^{3}TS 7/8** (SI 1), could be located. However, for the fragmentation of $[Ni(CH_3)(bipy)]^+$ all pathways (including singlet and triplet states) that lead to the elimination of methane are at least 65 kJ mol^{-1} higher in energy than the direct homolytic cleavage of the

Scheme 1. Generalized Mechanistic Scheme for the Fragmentations of Singlet $[M(X)(bipy)]^+$ (M = Ni, Pd, Pt; X = CH_3, Cl)

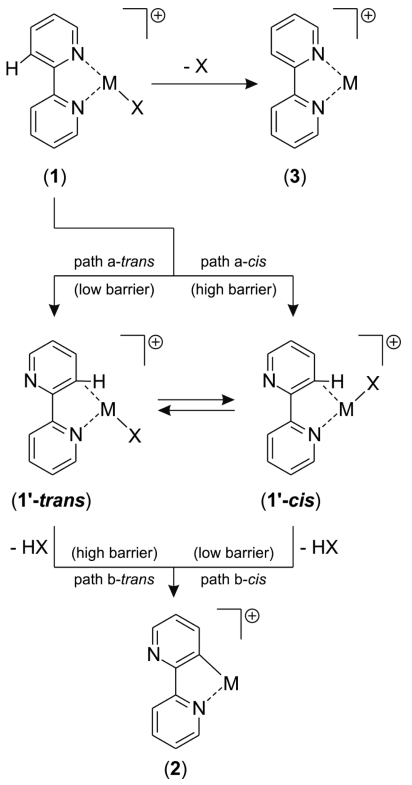

Table 3. Major Fragments in the CID of Mass-Selected $[M(Cl)(bipy)]^+$ (1-MCl) (M = Ni, Pd, Pt) at Various Collision Energies (E_{lab} in eV)[a]

	E_{lab}	1-MCl	− Cl	− HCl	− HCl/HCN	− Cl/bipy	− [M,Cl]	− [M,H,Cl]	− [M,H,Cl]/HCN	− C_5H_4NCl
1-NiCl	0	100	*>0*	**> 0**						
	5	100	*2*	**5**						
	10	100	*28*	**25**				**2**		2
	15	100	*53*	**27**				**7**		10
	20	100	*62*	**19**		*6*		**14**		21
	25	100	*51*	**14**		*19*		**24**		28
1-PdCl	0	100		**23**						
	5	92	*6*	**100**				**1**		
	10	42	*19*	**100**				**10**		
	15	53	*48*	**100**		*5*	*6*	**52**		
	20	84	*62*	**87**		*17*	*17*	**100**		
	25	73	*60*	**72**		*29*	*25*	**100**		
1-PtCl	0	100		**13**						
	5	100		**99**						
	10	73		**100**						
	15	42		**100**	**5**			**3**		
	20	30		**100**	**11**			**8**	**4**	
	25	55		**100**	**17**			**25**	**26**	

[a] Relative intensities are normalized to the base peak = 100. Numbers given in bold involve intramolecular C−H bond activation processes. Numbers in italics indicate simple ligand-loss processes.

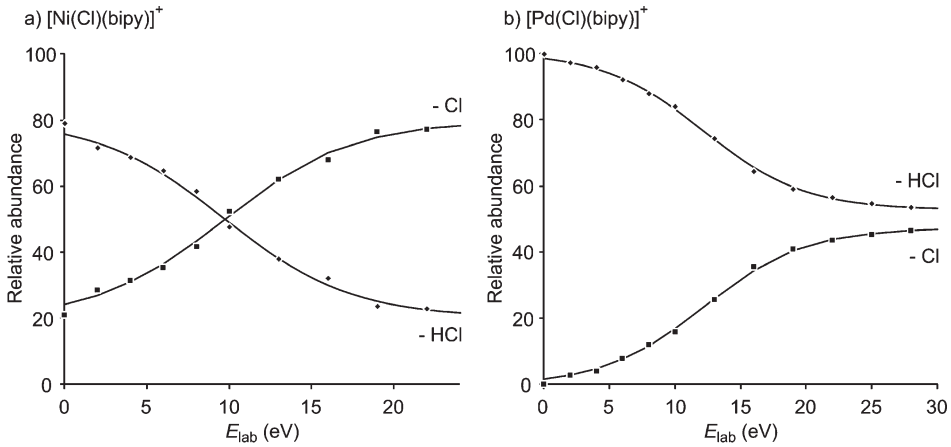

Figure 4. Relative intensities for the losses of HCl and Cl in the CIDs of mass-selected (a) [Ni(Cl)(bipy)]$^+$ and (b) [Pd(Cl)(bipy)]$^+$ at variable collision energies (E_{lab} in eV).

Ni$-$CH$_3$ bond, producing CH$_3$ and doublet **^{2}3-Ni** (the quartet-state structure **^{4}3-Ni** is even 131 kJ mol^{-1} higher in energy than **^{2}3-Ni**). These computational findings are in good agreement with the breakdown behavior of **1-NiMe**, as only CH$_3$ (but no CH$_4$) is lost upon CID. Also for [Pt(CH$_3$)(bipy)]$^+$, the experimental results are in keeping with the DFT results: elimination of CH$_4$ (via path a-*cis*, b-*cis*; Scheme 1) is predicted to be 58 kJ mol^{-1} more favored than direct cleavage of the Pt$-$CH$_3$ bond. The fact that even at higher collision energies no elimination of CH$_3$ is observed is due to the existence of an efficient channel for the competitive formation of neutral PtCH$_2$, as shown in Figure 2 (selected structures for this path are presented in Figure 3).[35] For [Pd(CH$_3$)(bipy)]$^+$, the C$-$H bond activation via **TS 10/11** (SI 2) corresponds to the rate-determining step in the formation of CH$_4$, which, according to the DFT results, is located only slightly above the methyl-elimination products **3-Pd** and CH$_3$. Within error bars, this is also reflected in the experimental results, as (minor) CH$_4$ elimination is observed only at low collision energies; due to a kinetic hindrance in the elimination of CH$_4$, this channel decreases when the collision energy is increased.[36]

Fragmentation of [M(Cl)(bipy)]$^+$ (M = Ni, Pd, Pt). Similar to the fragmentation of the methyl complex [Pt(CH$_3$)(bipy)]$^+$, upon CID of [Pt(Cl)(bipy)]$^+$ only neutral fragments are lost that contain a hydrogen atom from the bipy ligand (data in bold in Table 3). The most dominant channel corresponds to the formation of HCl, but at higher collision energies also the consecutive eliminations of HCl and HCN (due to the fragmentation of the (bipy $-$ H) ligand), the generation of neutral [Pt,H,Cl], and the consecutive eliminations of [Pt,H,Cl] and HCN take place. No homolytic cleavage of the Pt$-$Cl bond is observed. In the fragmentation of [3,3′-D$_2$]-**1-PtCl**, HCl and DCl are formed in a ratio of 3:97 (m/z = 391 $\rightarrow$ [D$_0$]:[D$_1$]:[D$_2$] = 0:3:97); this demonstrates that a hydrogen atom bound to C(3) or C(3′) serves as the exclusive source for the formation of hydrogen chloride ("rollover" cyclometalation).

In contrast to [Ni(CH$_3$)(bipy)]$^+$ and [Pd(CH$_3$)(bipy)]$^+$, the analogous chloride complexes [Ni(Cl)(bipy)]$^+$ and [Pd(Cl)(bipy)]$^+$ undergo intramolecular C$-$H bond activation concomitant with the elimination of HCl upon collision with xenon. In addition, homolytic cleavage of the M$-$Cl bond (M = Ni, Pd) takes place, and the ratio for the losses of HCl and Cl decreases with increasing collision energy for both complexes (Figure 4). This is a consequence of the fact that the formation of HCl is connected with several (tight) transition states (and is therefore kinetically hindered at higher collision energies), whereas scission of the M$-$Cl bond proceeds through a loose transition state.[36] On the basis of the branching ratios for HCl versus Cl formation, C$-$H bond activation is more efficient for the palladium than for the nickel complex, as clearly shown in Figure 4; this becomes also obvious from the fact that the signal for HCl loss in the CID spectrum of **1-PdCl** amounts to the base peak at E_{lab} = 5, 10, and 15 eV (Table 3). As to the regioselectivities of C$-$H bond activation associated with HCl loss, in the fragmentations of **1-NiCl** and **1-PdCl** the selectivity is not as high as for **1-PtCl**. This becomes obvious upon inspection of Table 4, which shows the C$-$H positions of bipy that are involved in HCl formation upon CID of **1-NiCl** and **1-PdCl** (the data given in the table are based on the ratios for the losses of HCl and DCl in the CID spectra of mass-selected [3,3′-D$_2$]-**1-NiCl**, [6,6′-D$_2$]-**1-NiCl**, [3,3′-D$_2$]-**1-PdCl**, and [6,6′-D$_2$]-**1-PdCl** at various collision energies E_{lab}; the complete set of data is given in the Supporting Information). For **1-NiCl**, abstraction of a hydrogen atom from position C(3), to form HCl, is below 70%; for **1-PdCl** it is below 90%, and upon increasing the collision energy, the selectivity for the abstraction of a hydrogen atom from a particular position of the bipy ligand decreases even further.

Table 4. Positions of the Hydrogen Atoms in bipy That Are Involved in the Formation of HCl upon CID of 1-NiCl and 1-PdCl at Various Collision Energies E_{lab} Based on the Data Shown in SI 8 without Accounting for Possible Kinetic Isotope Effects[a]

	position	5 eV	10 eV	15 eV	20 eV
1-NiCl	3		67	64	60
	4, 5		18	18	19
	6		15	18	21
1-PdCl	3	85	79	75	68
	4, 5	10	15	17	19
	6	5	6	8	13

[a] The distributions are normalized to $\sum$ = 100%.

---

[35] The analogous processes for the complexes **1-MMe** (M = Ni, Pd), e.g., the formations of ^{3}NiCH$_2$ + (bipy + H)$^+$ and PdCH$_2$ + (bipy + H)$^+$, require 373 and 279 kJ/mol, respectively; therefore, no competition exists with the losses of a methyl group from these complexes.

[36] Schröder, D.; Roithová, J.; Alikhani, E.; Kwapien, K.; Sauer, J. *Chem.—Eur. J.* **2010**, *16*, 4110.

Apart from the losses of HCl and Cl from **1-NiCl** and **1-PdCl**, elimination of neutral [M,H,Cl] as well as the combined losses of Cl and the bipy ligand is observed at increased collision energies. For **1-PdCl**, at higher collision energies neutral [Pd,Cl] is formed, and for **1-NiCl** the elimination of C_5H_4NCl points to cleavage of the C(2)−C(2′) bond of the heterocyclic ligand.

We have also performed DFT calculations for the processes defined in eqs 1 and 2 for the chloro complexes $[M(Cl)(bipy)]^+$ (M = Ni, Pd, Pt). The potential energy surfaces are shown in Figure 5, and selected structures are displayed in Figure 6 (the full set of structures is given in the Supporting Information). For the singlet states of **1-NiCl** and **1-PdCl**, due to the *trans* effect of the Cl ligand, initial rotation of the pyridyl ring *trans* to M−Cl (producing ^{1}**18** and **23**) is facilitated by 15 and 12 kJ mol^{-1}, respectively, compared with the rotation of the ring *cis* to the M−Cl bond; the latter leads to ^{1}**19** and **24** (the M−N bond *cis* to Cl in **1-MCl** is 0.035 and 0.042 Å shorter than that *trans* to Cl for M = Ni and Pd, respectively). However, the *trans* effect of a Cl ligand is weaker than that of a methyl group (Figures 1 and 3). For **1-PtCl**, only a transition state for the rotation of the pyridyl ring *trans* to the chloro ligand (**TS 1/27**) could be located. Interestingly, and in contrast with the methyl complexes **1-MMe** (M = Ni, Pd, Pt), the **1′-*trans*** structures (Scheme 1) ^{1}**18**, **23**, and **27** can easily isomerize to the **1′-*cis*** structures ^{1}**19**, **24**, and **28** (for the methyl complexes such a transition state could be located only for M = Pt; **TS 12/13**; 219 kJ mol^{-1}); only these **1′-*cis*** intermediates give rise to the formations of the HCl complexes ^{1}**20**, **26**, and **30**. For the transformation ^{1}**19** → ^{1}**20** (M = Ni), on the basis of the DFT findings a metathesis mechanism applies and the sequence **28** → **29** → **30** (M = Pt) proceeds via an OA/RE scenario. For M = Pd, transition states for both mechanisms could be located and the *σ*-bond metathesis pathway (**24** → **26**) is 24 kJ mol^{-1} higher in energy than the transition state for an oxidative addition (**24** → **25**). The triplet-state structure ^{3}**1-NiCl** is located 63 kJ mol^{-1} below the singlet-state species ^{1}**1-NiCl**, and similar to ^{3}**1-NiMe**, only one transition state (^{3}**TS 1/21**) for the pyridyl-ring rotation and one (^{3}**TS 21/22**) for the formation of the HCl complex ^{3}**22** via a metathesis pathway could be located.

However, the demands for the formation of HCl via "rollover" cyclometalation in both spin states are comparable, and HCl formation is predicted to be ca. 30 kJ mol^{-1} less favored than the formation of doublet ^{2}**3-Ni** concomitant with homolytic cleavage of the Ni−Cl bond; within error bars, this is reflected by the experimental results as both processes compete, with loss of the Cl ligand becoming dominant at higher E_{lab} values (Figure 4). The calculations on the fragmentation of $[Pd(Cl)(bipy)]^+$ predict HCl formation, when generated via a "rollover"-cyclometalation process, to be ca. 50 kJ mol^{-1} more favorable than direct Cl loss; moreover, the overall energy demand to bring about fragmentation is more than 100 kJ mol^{-1} lower for M = Pd than for M = Ni. These differences explain why intramolecular C−H bond activation is more efficient for **1-PdCl** than for **1-NiCl** and why **1-PdCl** already loses HCl at quite low collision energies (with only a small amount of Cl being formed); in contrast, **1-NiCl** eliminates HCl and Cl only at more elevated E_{lab} values. Also the fact that upon CID of $[Pt(Cl)(bipy)]^+$ no loss of Cl occurs is clearly reflected in the calculated PES, as the bond-dissociation energy of the Pt−Cl bond is calculated to be more than 120 kJ mol^{-1} higher than the energy required for the formation of HCl via "rollover" cyclometalation.

There is one interesting feature that deserves to be mentioned in passing. For both **1-PtMe** and **1-PtCl**, oxidative addition of Pt into the C(3)−H bond is energetically rather easy (compare **TS 13/14** and **TS 28/29**); especially, the barrier for **13** → **14** amounts to only 2 kJ mol^{-1}. In sharp contrast, barriers of at

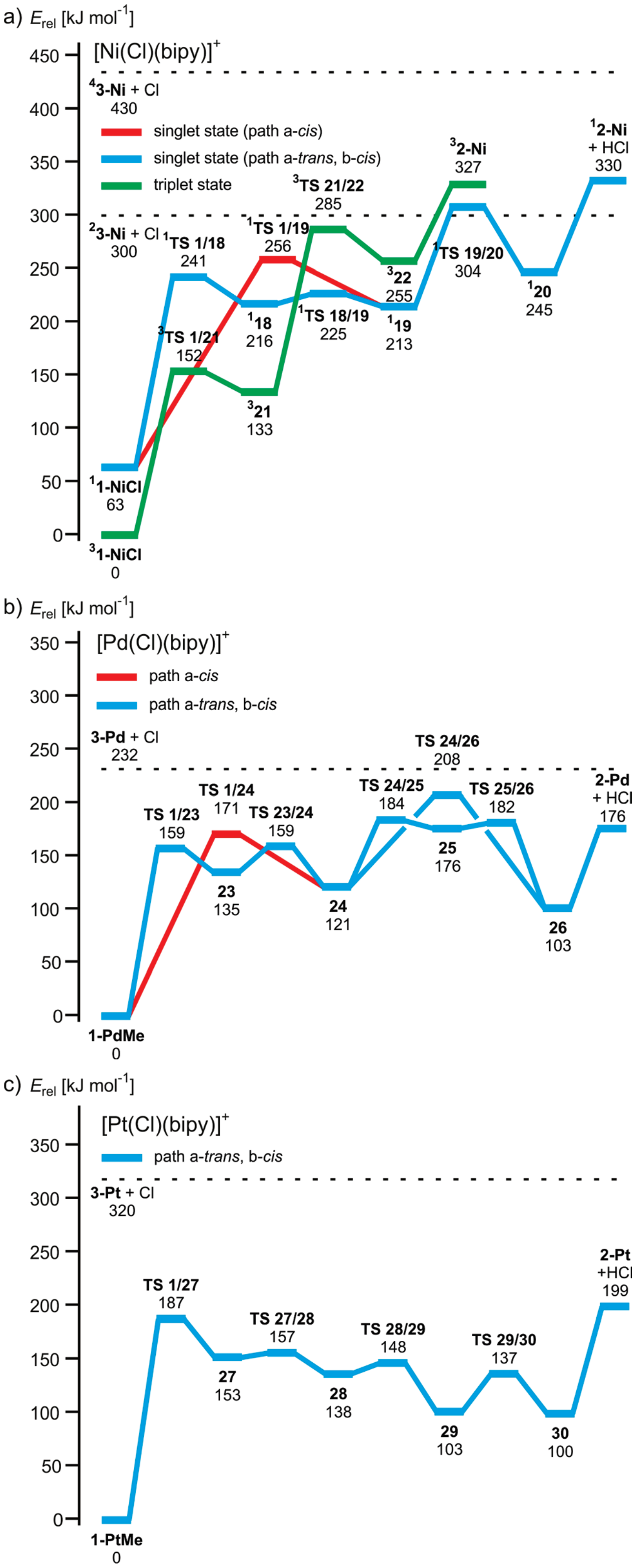

Figure 5. Schematic PESs for the fragmentations of $[M(Cl)(bipy)]^+$ (M = Ni, Pd, Pt) according to $[M(Cl)(bipy)]^+$ (**1-MCl**) → $[M(bipy - H)]^+$ (**2**) + HCl and $[M(Cl)(bipy)]^+$ (**1-MCl**) → $[M(bipy)]^+$ (**3**) + Cl based on DFT calculations using the B3LYP functional. For further explanations, see Scheme 1 and text.

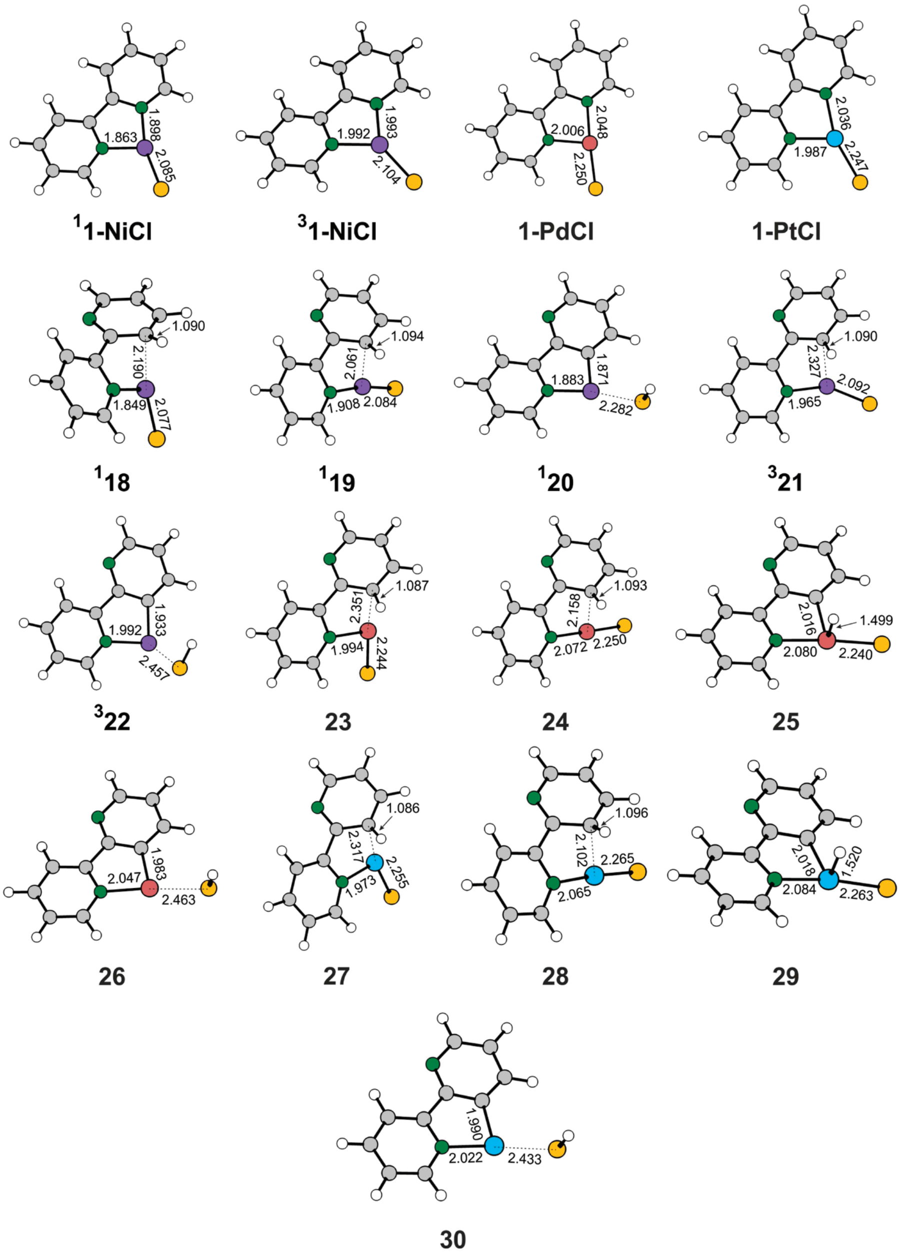

Figure 6. Geometry-optimized minimum structures of the species mentioned in Figure 5 together with relevant bond lengths (in Å) around the metal cores as calculated with the B3LYP functional.

least 54 kJ mol^{-1} have to be overcome in the C(3)$-$H bond activation steps for the systems **1-NiMe** and **1-NiCl** as well as for **1-PdMe** and **1-PdCl**, respectively.

Fragmentation of $[\mathrm{Ni(X)(bipy)}]^+$ (X = F, Cl, Br, I). As already discussed above, $[\mathrm{Ni(Cl)(bipy)}]^+$ eliminates HCl upon collision with Xe, while in the CID experiments with $[\mathrm{Ni(CH_3)(bipy)}]^+$ no intramolecular C$-$H bond activation is observed at all. Therefore, we were interested in the fragmentation patterns of analogous nickel-halogen complexes subjected to similar conditions. The results are summarized in Table 5. Only **1-NiF** and **1-NiCl** lose HX upon CID. This process as well as the elimination of neutral [Ni,H,X] is slightly more efficient for **1-NiF** than for **1-NiCl**. Moreover, in contrast to **1-NiCl**, **1-NiF** does not undergo homolytic cleavage of the Ni$-$F bond upon collision. Common to both complexes is the formation of C_5H_4NX (X = F, Cl), which, however, is more pronounced for X = F. Interestingly, **1-NiF** exhibits a high selectivity in the formation of HF: [3,3′-D_2]-**1-NiF** loses HF and DF in a ratio of 96:4; in contrast, CID of [6,6′-D_2]-**1-NiF** at 10 eV results in the eliminations of HF and DF in a ratio of 8:92. This translates into abstraction of hydrogen atoms from positions 3, 4 or 5, and 6 in a ratio of 4:4:92. Obviously, near to no "rollover" cyclometalation occurs for the Ni complex, but the C$-$H bond atom next to the nitrogen atom of bipy is attacked preferentially. We have initiated computational investigations on mechanisms that could possibly explain the highly selective abstraction of a hydrogen atom from position C(6) of bipyridine in the fragmentation of **1-NiF**; however, we did not yet succeed in finding a completely satisfying potential-energy surface that accounts for all experimental observations.

Upon CID of **1-NiBr** and **1-NiI**, no products due to C$-$H bond activation are observed. Obviously the Ni$-$X bonds (X = Br, I) are so weak that the sequence of decomplexation, rotation of a pyridyl ring, and C$-$H bond activation cannot

Table 5. Major Fragments in the CID of Mass-Selected $[Ni(X)(bipy)]^+$ (1-NiX) Complexes (X = F, Cl, Br, I) at Various Collision Energies (E_{lab} in eV)[a]

	E_{lab}	1-NiX	− X	− HX	− X/bipy	− [Ni,H,X]	− C_5H_4NX
1-NiF	0	100		**1**			
	5	100		**13**			
	10	100		**55**		**8**	6
	15	100		**50**		**18**	38
	20	100		**31**		**25**	76
	25	100		**18**		**28**	83
1-NiCl	0	100	*>0*	**>0**			
	5	100	*2*	**5**			
	10	100	*28*	**25**		**2**	2
	15	100	*53*	**27**		**7**	10
	20	100	*62*	**19**	*6*	**14**	21
	25	100	*51*	**14**	*19*	**24**	28
1-NiBr	0	100	*9*				
	5	100	*35*				
	10	72	*100*				
	15	30	*100*				
	20	36	*100*		*6*		
	25	52	*100*		*24*		
1-NiI	0	100	*9*				
	5	74	*100*				
	10	30	*100*				
	15	11	*100*				
	20	12	*100*		*2*		
	25	20	*100*		*8*		

[a] Relative intensities are normalized to the base peak = 100. Numbers given in bold involve intramolecular C−H bond activation processes. Numbers in italics indicate simple ligand-loss processes.

Table 6. Major Fragments in the CID of Mass-Selected $[M(OAc)(bipy)]^+$ (1-MOAc) (M = Ni, Pd) at Various Collision Energies (E_{lab} in eV)[a]

	E_{lab}	1-MOAc	− $AcO^•$	− $AcO^•$/bipy	− CO_2
1-NiOAc	0	100	*>0*		>0
	5	100	*11*		6
	10	93	*100*		12
	15	38	*100*		4
	20	43	*100*		2
	25	40	*100*		2
1-PdOAc	0	100	*1*		5
	5	100	*33*		29
	10	74	*100*		29
	15	28	*100*		11
	20	32	*100*	*8*	8
	25	39	*100*	*20*	8

[a] Relative intensities are normalized to the base peak = 100. Numbers in italics indicate simple ligand-loss processes.

compete with the direct ligand loss, being the only event observed at moderate collision energies. At higher collision energies, the consecutive eliminations of X and bipy take place. As expected, at a given energy, loss of X from $[Ni(X)(bipy)]^+$ is more dominant for X = I than for X = Br.

Fragmentation of $[M(OAc)(bipy)]^+$ (M = Ni, Pd). Palladium acetate is frequently used in synthetic protocols to generate cyclometalated palladium complexes. Therefore, we were interested to see if acetate could also serve as an appropriate ligand to bring about "rollover" cyclometalation in the gas phase. However, as shown in Table 6, acetate is too weakly bound to the metal center in **1-NiOAc** and **1-PdOAc**, and upon CID, homolytic cleavage of the M−OAc bond prevails. No C−H bond activation processes are observed. At slightly higher collision energies, the acetate complexes lose neutral CO_2 and, quite likely, the corresponding methyl complexes **1-NiMe** and **1-PdMe** are concomitantly formed (for analogous examples see ref 37).

Conclusions

The branching ratios and the mechanistic details of the gas-phase fragmentations of $[M(X)(bipy)]^+$ (bipy = 2,2′-bipyridine) complexes depend strongly on the nature of the metal M (M = Ni, Pd, Pt) as well as that of the ligand X (X = CH_3, F, Cl, Br, I, OAc). Only the $[Pt(CH_3)(bipy)]^+$ and $[Pt(Cl)(bipy)]^+$ complexes selectively and exclusively undergo losses of HX (X = CH_3, Cl), resulting in the formation of "rollover"-cyclometalated $[Pt(bipy - H)]^+$. Upon low-energy collisions with xenon, $[Ni(CH_3)(bipy)]^+$ and $[Pd(CH_3)(bipy)]^+$ undergo homolytic cleavage of the M−CH_3 bond, and also from $[Ni(Br)(bipy)]^+$, $[Ni(I)(bipy)]^+$, $[Ni(OAc)(bipy)]^+$, and $[Pd(OAc)(bipy)]^+$ the neutral nonheterocyclic ligand is eliminated as a radical X (X = Br, I, OAc); any C−H bond activation processes are absent. However, the scenarios for the fragmentations of $[Pd(Cl)(bipy)]^+$, $[Ni(Cl)(bipy)]^+$, and $[Ni(F)(bipy)]^+$ are more subtle. For all three substrates, in addition to the homolytic cleavage of the M−X bond observed for $[Pd(Cl)(bipy)]^+$ and $[Ni(Cl)(bipy)]^+$, HX (X = F, Cl) is formed upon CID; however, the site selectivity for the hydrogen-atom abstraction from the bipy ligand varies: for $[Pd(Cl)(bipy)]^+$ and $[Ni(Cl)(bipy)]^+$ the hydrogen atom originates predominantly from position C(3), while for $[Ni(F)(bipy)]^+$ position C(6) serves as the main hydrogen source. The product distributions in the fragmentations of $[M(X)(bipy)]^+$ with M = Ni, Pd, Pt and X = CH_3, Cl are quite straightforwardly explained by DFT calculations. The *trans* effect of the nonheterocyclic ligand (especially for X = CH_3) has a strong influence on the preferred pathway in the course of the "rollover"-cyclometalation scenario. A metathesis-like mechanism is predicted to be operative for M = Ni, and an OA/RE pathway for M = Pt. For palladium, the preferred mechanism depends on the nature of the ligand X, and for X = Cl, an OA/RE pathway is slightly preferred energetically.

Acknowledgment. We thank Dr. Xinhao Zhang for enlightening discussions and are grateful for financial support to the Fonds der Chemischen Industrie as well as the Cluster of Excellence "Unifying Concepts in Catalysis" coordinated by the Technische Universität Berlin and funded by the Deutsche Forschungsgemeinschaft.

Supporting Information Available: A summary of all computed structures is available free of charge via the Internet at http://pubs.acs.org.

---

(37) (a) Rijs, N.; Khairallah, G. N.; Waters, T.; O'Hair, R. A. J. *J. Am. Chem. Soc.* **2008**, *130*, 1069. (b) Rijs, N. J.; O'Hair, R. A. J. *Organometallics* **2009**, *28*, 2684. (c) Rijs, N. J.; Sanvido, G. B.; Khairallah, G. N.; O'Hair, R. A. J. *Dalton Trans.* **2010**, *39*, 8655.